

# Role of Hypoxic Secretome from Mesenchymal Stem Cells in Enhancing Tissue Repair: Regulatory Effects on HIF-1 $\alpha$ , VEGF, and Fibroblast in a Sphincterotomy Rat Model

Leecarlo Millano Lumban Gaol<sup>1-3</sup>, Ambrosius Purba<sup>1</sup>, Rizki Diposarosa<sup>1,2</sup>, Yuni Susanti Pratiwi<sup>1</sup>

<sup>1</sup>Faculty of Medicine Padjadjaran University, Bandung, Indonesia; <sup>2</sup>Dr. Hasan Sadikin General Hospital, Bandung, Indonesia; <sup>3</sup>Faculty of Medicine Krida Wacana Christian University, Jakarta, Indonesia

Correspondence: Leecarlo Millano Lumban Gaol, Faculty of Medicine Padjadjaran University, Raya Bandung Sumedang Street No. 21, Hegarmanah, Jatinangor, Sumedang, Bandung, West Java, 45363, Indonesia, Email millanoleecarlo@gmail.com

**Background:** Fecal incontinence (FI) is the inability to control bowel movements, resulting in fecal leakage. If left untreated, FI can seriously impact the long-term well-being of individuals affected. Recently, using secretome has become a promising new treatment method. The secretome combines growth factors released outside cells during stem cell development, such as mesenchymal stem cells. It consists of soluble proteins, nucleic acids, fats, and extracellular vesicles, which contribute to different cell processes. The primary aim is to assess the impact of hypoxic secretome administration on accelerating wound healing through the HIF-1 $\alpha$  pathway in a post-sphincterotomy rat model.

**Methods:** The study was conducted with two distinct groups of 10 rats each, the control and treatment groups, which were injected with hypoxic secretome at 0.3 mL. The inclusion criteria for the rats were as follows: male gender, belonging to the Sprague-Dawley strain, aged between 12 to 16 weeks, with an average body weight ranging from 240 to 250 grams.

**Results:** There was an increase in HIF-1 $\alpha$  gene expression in both groups. The treatment group 37 was significantly higher on day 42 ( $p = 0.001$ ). VEGF increased significantly in the treatment 38 group on day 42 ( $p = 0.015$ ). The neovascularization score increased significantly in the treatment 39 group during the first 24 hours ( $p = 0.004$ ). The fibroblast score increased significantly in the 40 treatment group in the first 24 hours ( $p = 0.000$ ) and 42 days ( $p = 0.035$ ). After being given secretome, there was a higher increase in % collagen area and collagen area ( $\mu\text{m}^2$ ) in the treatment group compared to the control group (27,77 vs 11.01) and (419.027,66 vs 186.694,16).

**Conclusion:** The use of hypoxic secretome has a significant effect as a choice for the treatment of anal sphincter injury after sphincterotomy through the HIF-1 $\alpha$ -VEGF-Fibroblast pathway.

**Keywords:** fecal incontinence, fibroblast, HIF-1 $\alpha$ , hypoxic secretome, neovascularization, VEGF

## Introduction

Fecal incontinence (FI) is an involuntary passage of liquid and/or solid feces that negatively affects the quality of life, with prevalence ranging from 7% to 15% in the general population.<sup>1</sup> In patients with fecal incontinence, various physical and psychological disorders can occur, such as recurrent infections, ulcers and skin scars, social anxiety disorders, behavioral problems, self-deprecation or isolation, and other problems that give rise to feelings of guilt and shame.<sup>2-4</sup> FI can begin in childhood and persist into adulthood. Among children, the incidence rates of FI vary from 1.6% to 4.4%, and boys have more potential to suffer from fecal incontinence.<sup>5</sup> The leading cause is often associated with surgeries such as internal sphincterotomy and fistulotomy, which account for 35–45% of FI occurrences.<sup>6-8</sup>

Various efforts have been made to prevent FI after surgical procedures, including conventional therapies like enema use, neurostimulation/biofeedback, and reoperation. However, the outcomes of these methods have often been

unsatisfactory, leading to persistent FI, surgical wound infections, rectal prolapse, and other complications.<sup>9</sup> Anoplasty alone is not compelling enough to achieve reasonable recovery rates for anorectal anomalies to prevent FI in children. Research in Indonesia reported that the incidence of fecal incontinence caused by complications from Posterosagittal Anorectoplasty (PSARP) surgery in children with anorectal malformations is 5.8%.<sup>10</sup> After anoplasty, different supplementary therapies have been tried to enhance recovery rates. Still, conservative methods have not produced optimal results yet.<sup>11–13</sup>

The secretome, composed of cytokines, proteins, chemokines, extracellular vesicles, and growth factors released by Mesenchymal Stem Cells (MSCs), has shown significant promise in tissue repair and regeneration.<sup>14</sup> Wound treatment with the secretome can significantly accelerate new tissue formation, collagen deposition, and re-epithelialization, which is mediated by growth factors such as vascular endothelial growth factor (VEGF).<sup>15</sup> VEGF expression is associated with hypoxia-inducible factor 1 (HIF-1) and induced by hypoxia through an HIF-1 $\alpha$  independent pathway.<sup>16</sup> To promote the expression of VEGF in hypoxic conditions, HIF-1 $\alpha$  will bind to HIF-1 $\beta$  to form the active transcription factor HIF-1. This transcription factor will then translocate to the nucleus and bind to hypoxia regulatory elements (HREs) within the promoter region of HIF-1-inducible genes in conjunction with coactivators p300 and CREB-binding protein (CBP).<sup>17</sup> Xi et al conducted research that resulted in the secretome having the most important role in the proliferation stage of wound healing, which upregulates VEGF and accelerates the transformation of fibroblasts into myofibroblasts, thereby increasing collagen synthesis.<sup>18</sup>

This process highlights the essential role of HIF-1 $\alpha$  in activating the VEGF gene, promoting angiogenesis during the wound healing process, inducing fibroblast activity, promoting migration, and the formation of the extracellular matrix.<sup>19</sup> There has not been much research discussing the role of the secretome in wound healing in sphincterotomy rat models. Utilizing the secretome as a treatment for FI is a novel approach that is expected to increase recovery rates and produce optimal results compared with conservative methods. The main aim of this research is to examine the role of the secretome, especially VEGF, in accelerating tissue repair through the HIF-1 $\alpha$ /VEGF pathways and its relation to the formation of fibroblasts in muscles in post-sphincterotomy mouse models.

## Materials and Methods

### Place and Ethical Clearance of Research

The maintenance of rats in this research was carried out at the Laboratory of the Faculty of Veterinary Medicine, Bogor Agricultural University, West Java. Institutional Animal Care approved this experiment and Use Committees (IACUC) (630/UN6.KEP/EC/2022) of the Faculty of Medicine, Padjadjaran.

### Research Design and Subject

Twenty male rats of the Sprague-Dawley aged between 12 and 16 weeks with weights ranging from 240 to 250 grams were taken for an experimental interventional with a randomized pre- and post-test with a control group design. This study was conducted with two distinct groups, the control and treatment groups, each consisting of 10 rats. The rats were sourced from the same breeding grounds, received the same feed, and were healthy, showing regular activity and behavior. The rats that looked sick (inactivity, fur looks dull, loose stools, bite wounds), had more than >10% weight loss during adaptation, and died before treatment were excluded from the research. Furthermore, the maintenance of rats was carried out for two weeks. Sprague-Dawley was chosen because this strain of rats was the most widely used in the laboratory and had advantages in terms of availability, ease of breeding, congenic strains, and high resistance. A study showed that this commonly used mouse strain had an anal sphincter structure similar to humans.<sup>20</sup>

The entire research subject underwent microscopic surgery that damaged 25% of the sphincter ani muscle. Before surgery, the rats were anesthetized with intramuscular injection of ketamine and intraperitoneal injection of xylazine hydrochloride (0.15 mL/kg). The internal and external anal sphincter muscles were separated, and incisions were made at 10 o'clock and 2 o'clock positions using surgical techniques under a microscope.

Fecal incontinence was evaluated through the analysis of rat feces, which were classified as Bristol type 6–7. This classification indicates the presence of fecal incontinence, as the observed fecal matter was loose and watery.

## Secretome Preparation and Isolation

This research used the secretome of human umbilical cord mesenchymal stem cells (SM-hUCMSC) as the intervention. Mesenchymal stem cells from the umbilical cord were isolated and cultured up to passage 6 in a T175 Flask. Once reaching 70–80% confluence, the culture medium was replaced with a basal medium and incubated under hypoxic conditions (5% O<sub>2</sub>) at 37°C for 72 hours to allow secretion of the secretome. The conditioned medium (CM) was frozen at –80°C for a week. The results of the analysis of active substance content based on ELISA tests revealed pro-collagen levels at 655,100.00 pg/mL, vascular endothelial growth factor (VEGF) at 21.42 pg/mL, and basic fibroblast growth factor (bFGF) at 34.64 pg/mL.

For the secretome isolation, the umbilical cord is placed into a 500 mL Schott bottle containing a cold transport medium ( $\alpha$ -MEM + 1% ABAM). The umbilical cord is then washed using sterile PBS (pH 7.4) in a sterile tea strainer placed over a 500 mL beaker, performing 3–4 washes until the PBS solution remains clear or unchanged in color. This process removes contaminants from the specimen, and the contaminant solution is discarded. The washed specimen is transferred into several 50 mL tubes, with each tube filled to a maximum of 15 mL. An equal volume of 0.075% collagenase (30 mL) is added to the samples (1 part sample to 2 parts collagenase). The samples, now containing collagenase, will form two phases. Incubate in 5% CO<sub>2</sub> at 37°C for 1 hour, homogenizing every 15 minutes. After 1 hour, two layers will form: the upper layer is discarded using a pipette, and the lower layer is collected, pipetted into a 15 mL centrifuge tube, and filtered using a 100  $\mu$ m cell strainer. The sample is then transferred to several 15 mL tubes and centrifuged at 1200 rpm for 10 minutes at room temperature. After centrifugation, the supernatant is discarded, and 10 mL of lysis buffer (resuspension) is added to remove red cell debris. The sample is centrifuged again at 1200 rpm for 10 minutes. The supernatant is discarded, and the pellet is resuspended in 1 mL of complete growth medium and transferred into a T-25 flask. Incubate at 5% CO<sub>2</sub>, 37°C. Observe the cells and replace the medium every 2–3 days or when the medium changes color. Replace the medium 2–3 times a week until the cells reach 80% confluency. Once the cells reach 80% confluency, they are subcultured.

## Cryopreservation

The isolated cells are placed into cryovials and stored at –20°C for 30–60 minutes. Subsequently, they are transferred to –80°C for overnight storage and then kept in a cryo tank at –196°C.

## Thawing

To thaw the mesenchymal stem cells (MSCs), remove the vial from the liquid nitrogen tank (–196°C) and melt it in a 37°C water bath until the frozen suspension becomes liquid. Transfer the cells into a 15 mL tube containing 4 mL of complete medium (DMEM + 10% Fetal Fetal Plasma, FFP). Centrifuge at 1600 rpm for 5 minutes. Discard the supernatant, resuspend the pellet in 5 mL of culture medium, and transfer to a T25 culture flask. Incubate in a 37°C, 5% CO<sub>2</sub> incubator, observing daily with an inverted microscope. Every 2–3 days, or when the medium turns yellow, replace the old medium with the fresh medium by washing the culture with PBS. Continue incubation until the cells reach 70% confluency in the T25 flask. When the cells reach 70–80% confluency, wash with PBS. Add 1 mL of 0.25% trypsin to the culture flask and incubate for approximately 5 minutes to detach the cells from the T25 flask. Confirm cell detachment using an inverted microscope. To stop the trypsinization, add 1 mL of complete medium to the flask, transfer the entire content to a 15 mL tube, and centrifuge at 1600 rpm for 5 minutes. Discard the supernatant and resuspend the pellet in 1 mL of complete medium with added serum (FFP).

## Cell Harvesting and Characterization

When the cells reach 70–80% confluency, wash them with PBS to remove any residual medium. Add 1 mL of 0.25% trypsin to the culture flask and incubate for approximately 5 minutes to detach the cells from the T25 surface. Check the cells under a microscope to confirm that they have fully detached. For thorough confirmation, use an inverted microscope. After detaching the cells, add 1 mL of complete medium to neutralize the trypsin. Transfer the contents of the T25

flask into a 15 mL centrifuge tube and centrifuge at 1600 rpm for 5 minutes. Discard the supernatant and resuspend the pellet in 1 mL of complete medium supplemented with Fetal Fetal Plasma (FFP).

## Characterizing Adipose-Derived Mesenchymal Stem Cells

Adipose-derived mesenchymal stem cells (MSCs) are characterized through immunophenotyping. This method involves assessing the expression of specific Cluster of Differentiation (CD) markers: positive for CD73, CD90, CD105, and CD44 and negative for CD11b, CD19, CD34, CD45, and HLA-DR. The analysis is carried out using a flow cytometer.

### Immunophenotyping Procedure

1. Prepare nine 1.5 mL tubes, each for a different component of the hMSCs characterization process.
2. Add 100  $\mu$ L of hMSCs suspension to each tube.
3. Incubate the tubes in the dark for 30 minutes.
4. Wash the stained cells twice with PBS.
5. Analyze the cells using a flow cytometer.

### Protein Quantification

To measure protein levels, mix 10  $\mu$ L of conditioned medium and MEM- $\alpha$  with 190  $\mu$ L of Coomassie Brilliant Blue G-250 reagent. Vortex the mixture to ensure thorough homogenization, then transfer it to a 96-well plate. Measure the absorbance at 600 nm using an ELISA reader. Perform the assay in duplicate and determine the protein concentration using a standard BSA curve.

### Preparing the BSA Standard Curve

Dissolve 100 mg of Bovine Serum Albumin (BSA) in a 10 mL volumetric flask with distilled water to obtain a stock solution with a concentration of 10  $\mu$ g/ $\mu$ L. From this stock solution, prepare serial dilutions to achieve concentrations of 0.5, 0.75, 1.0, and 1.25  $\mu$ g/ $\mu$ L. Pipette 10  $\mu$ L of each dilution into 190  $\mu$ L of Coomassie Brilliant Blue G-250 reagent, vortex to mix, and transfer to a 96-well plate. Measure the absorbance at 600 nm using an ELISA reader and generate a standard curve with absorbance on the y-axis and concentration on the x-axis.

### Gel Preparation

Weigh Hydroxypropyl Methylcellulose (HPMC) and disperse it in hot water. Allow it to sit covered for 24 hours to expand. Once expanded, mix in 10% propylene glycol and 0.3% Glydant<sup>®</sup> Plus Liquid while stirring. Slowly incorporate this mixture into the conditioned medium to achieve a final protein concentration of 0.05%. Stir the mixture in a cold environment using an ice bath until a homogeneous gel forms. Finally, add demineralized water to reach a total volume of 100%.

## Subject Intervention

In the treatment group, hypoxic secretome was administered. Secretome is injected directly after sphincterotomy at 0.3 mL and injected into the sphincter ani muscle at three points: 12 o'clock, 4 o'clock, and 8 o'clock. The control group received a standard saline solution at 0.3 mL. Meanwhile, the pretest group underwent termination directly without any treatment.<sup>21</sup>

## RNA Extraction

The extraction of mRNA for HIF-1 $\alpha$ , VEGF, and  $\beta$ -actin was carried out using TRIReagent following the manufacturer's protocol (Molecular Research Center Inc., Cincinnati, OH). After extraction, the RNA concentration and purity were determined using a spectrophotometer. For qPCR, the cDNA synthesis was performed using a reverse transcription kit (Promega Corporation, Madison, WI), where 1  $\mu$ g of total RNA was reverse transcribed in a 20  $\mu$ L reaction mixture containing oligo(dT) primers and reverse transcriptase.

The qPCR was conducted using a 96-well plate format in a real-time PCR system (eg, Bio-Rad CFX96). The primers used for amplifying the HIF-1 $\alpha$ , VEGF, and  $\beta$ -actin genes were as follows: HIF-1 $\alpha$  forward primer 5'-TGCTC



ATCAGTTGCCACTTC-3', reverse primer 5'-TGGGCCATTCTGTGTGTAA-3'; VEGF forward primer 5'-ACTGGACCCTGGCTTTACTG-3', reverse primer 5'-TCTGCTCTCCTTCTGTCGTG-3'; and  $\beta$ -actin (ACTB) forward primer 5'-CCTGTGCTGCTCACCAGGC-3', reverse primer 5'-GACCCCGTCTCTCCGGAGTCCATC-3'. These primers amplify fragments of 209 bp for HIF-1 $\alpha$ , 150 bp for VEGF, and 153 bp for  $\beta$ -actin.

Each 20  $\mu$ L qPCR reaction contained 1  $\mu$ L of cDNA, 10  $\mu$ L of SYBR Green qPCR Master Mix (Applied Biosystems, Foster City, CA), 0.5  $\mu$ L of each primer (10  $\mu$ M), and 8  $\mu$ L of nuclease-free water. The cycling conditions included an initial denaturation at 95°C for 3 minutes, followed by 40 cycles of denaturation at 95°C for 15 seconds, annealing at 60°C for 30 seconds, and extension at 72°C for 30 seconds. A melt curve analysis was performed at the end of the run to confirm the specificity of the amplification.

Relative gene expression was calculated using the comparative threshold cycle (CT) method. The CT values of HIF-1 $\alpha$  and VEGF were normalized to the housekeeping gene  $\beta$ -actin. The fold change in expression was determined using the  $2^{-\Delta\Delta CT}$  method, where  $\Delta CT$  represents the difference between the target gene and  $\beta$ -actin, and  $\Delta\Delta CT$  represents the difference in  $\Delta CT$  between treated and control samples. Each experiment was performed in triplicate to ensure reproducibility and no-template controls were included to rule out contamination.

## Real-Time Quantitative PCR (q-RT-PCR)

The synthesis of cDNA is performed using reverse transcriptase enzyme and oligo dT primers, which will bind to the poly-A tail region characteristic of mRNA. This is done to amplify the mRNA used during PCR analysis. The synthesis of cDNA involves several steps, including the isolation of mRNA to be used, visualization using electrophoresis, synthesis of the first strand cDNA, and amplification of the obtained cDNA. The analysis of mRNA expression of HIF-1 $\alpha$ , VEGF was conducted using the qRT-PCR method with Mini Opticon<sup>®</sup> Real-Time PCR and the One Step RT-PCR kit. Beta-actin was utilized as the reference gene because its expression is not influenced by treatment on the anal sphincter muscle. The amplification conditions were as follows: 2 min preincubation at 50°C, 10 min at 95°C for enzyme activation, and 40 cycles at 94°C denaturation for 10s, 55°C annealing for 20s, and 72°C extension for 20s. Comparative threshold cycle (Ct) technique. The primers used were: HIF-1 $\alpha$ -forward primer, TGCTCATCAGTTGCCACTTC, HIF-1 $\alpha$ -reverse primer, TGGGCCATTCTGTGTGTAA,<sup>22</sup> VEGF-forward primer, ACTGGACCCTGGCTTTACTG, VEGF-reverse primer, TCTGCTCTCCTTCTGTCGTG,<sup>23</sup> and ACTB forward primer, CCTGTGCTGCTCACCAGGC, and ACTB reverse primer GACCCCGTCTCTCCGGAGTCCATC.<sup>20</sup>

In this PCR analysis, the following tools and materials are utilized:

- RNA Extraction Kit: DirectZol RNA Kit, Zymo Research, California
- Reverse transcription: cDNA Synthesis System, Biotline, United Kingdom
- PCR Real-Time Machine: PCX Opus, Biorad, California
- Master Mix: SsoFast EvaGreen Supermix, Biorad, California

## Histological Analysis

At 24 hours and the 42 days post-surgery, rats were euthanized using a lethal dose of ketamine that was 50 mg/kgBW and Xylazine 10 mg/kgBW injected intramuscularly, and surgery was performed on the anal sphincter for histological analysis. The anal sphincter muscle tissue of rats was extracted coronally, targeting the area between the damaged sphincters.

Samples of descending colon tissue were collected to assess regional side effects on glandular tissue surrounding the colon. The collected tissue was fixed for 24 hours in 4% paraformaldehyde, followed by 48 hours of decalcification in Morse solution (10% sodium citrate and 22.5% formic acid) at 4°C. After dehydration in graded ethanol, the tissue was embedded in paraffin blocks. Coronal sections (5 micrometers) were stained with hematoxylin-eosin (HE) and observed under an Olympus BH-2 light microscope equipped with a DP70 camera.

The effect of the secretome on neovascularization and fibrosis during tissue repair following sphincterotomy was assessed histologically using HE staining. The histology score for neovascularization and fibrosis assessment is determined using the Textor criteria, where each sample was evaluated in four distinct fields of view by three

independent observers. A score of 1 indicates that the fibrosis area is less than 25%. A score of 2 indicates that the fibrosis area is between 25% and 50%. A score of 3 indicates that the fibrosis area is between 50% and 75%. Finally, a score of 4 indicates that the fibrosis area is greater than 75% on average across four fields.<sup>24</sup>

The impact of the secretome on fibroblast during tissue repair was evaluated using HE staining at the histological level. The histology score for fibroblast assessment is determined using the Guo criteria. A score of 0 indicates that no fibroblastic cells were detected in the entire field of view, and 1 indicates that the fibroblasts are rarely found and are distributed sporadically. A score of 2 indicates that the fibroblasts are seen more frequently but are not dominant. A score of 3 indicates that the Fibroblasts dominate the visual field, but there is still free space. Finally, a score of 4 indicates that the fibroblasts almost or fill the visual field.<sup>25</sup>

The impact of the secretome on the collagen area was evaluated using Masson Trichrome staining at the histological level. The collagen area was analyzed using Image-J software, demonstrating the difference in % collagen area and collagen area density.

## Statistical Analysis

Each value was expressed as the mean standard deviation. To determine the differences among the three independent groups, the Mann–Whitney and Kruskal–Wallis tests were applied to the differences between the two independent groups. The statistical analysis utilized Statistical Package for the Social Sciences (SPSS) v.26, and the confidence interval was 95%. Values were deemed to be statistically significant at  $p < 0.05$ .

## Results

Twenty rats were used as research subjects, all undergoing a 2-week acclimatization period 183 and receiving regular care and feeding without special treatment. After this period, the rats were induced to become a fecal incontinence model, with ten rats assigned to the treatment group and ten to the control group. However, two rats dropped out of the study, with one dying during surgery 186 and the other passing away one day after the procedure (Figure 1).

The study showed that HIF-1 $\alpha$  expression in the control group at 24 hours was not significantly higher than in the treatment group at 24 hours ( $24.93 \pm 0.43$  vs  $24.72 \pm 0.42$ ,  $p = 0.47$ ) and HIF-1 $\alpha$  expression in the control group at 42 days was not significantly higher than the control group at 24 hours ( $26.16 \pm 0.66$  vs  $24.93 \pm 0.43$ ,  $p = 0.06$ ). There was a difference in the expression of the HIF-1 $\alpha$  expression between the control group and the treatment group (Figure 2).

The results of the analysis showed that after being given secretome, the study showed that HIF-1 $\alpha$  expression in the treatment group at 42 days was significantly higher than the control group at 42 days ( $27.82 \pm 0.67$  vs  $26.16 \pm 0.65$ ,  $p = 0.01$ ) and HIF-1 $\alpha$  expression in the treatment group at 42 days was not significantly higher than treatment group at 24 hours ( $27.82 \pm 0.67$  vs  $24.73 \pm 0.41$ ,  $p = 0.06$ ). There was a difference in the expression of the HIF-1 $\alpha$  expression between the control group and the treatment group (Figure 3).

There was an increase of HIF-1 $\alpha$  expression where the treatment group with secretome administration was significantly higher than the control group ( $3.20 \pm 0.59$  vs  $1.16 \pm 0.35$ ,  $p < 0.01$ ), indicating that there was an effect of secretome between the control group and treatment group on the increase of HIF-1 $\alpha$  expression in a fecal incontinence rat model.

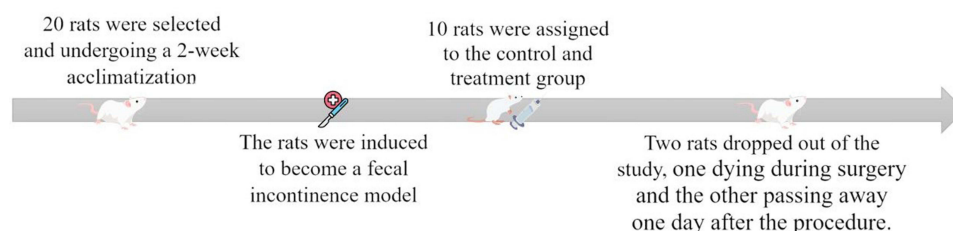


**Figure 1** The procedure of the Rats.

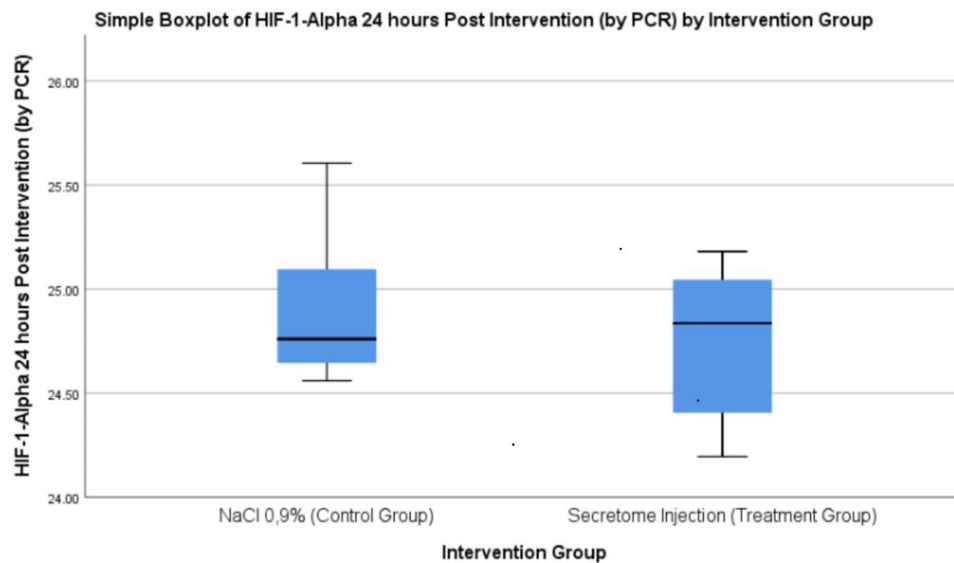


**Figure 2** HIF-1 $\alpha$  expression in 24 hours Control Group (left) Treatment Group (right).

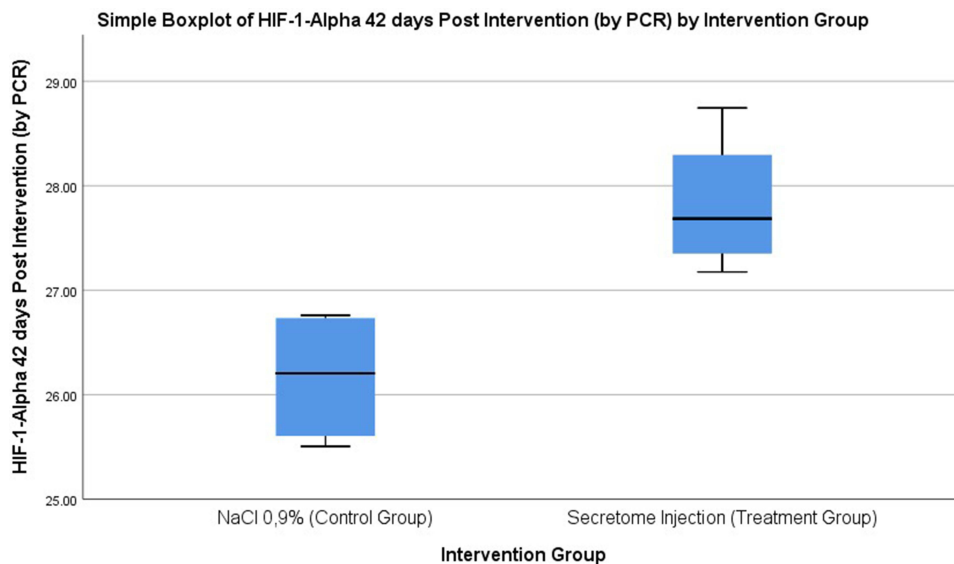


**Figure 3** HIF-1 $\alpha$  expression in 42 days Control Group (left) Treatment Group (right).

The study showed that VEGF expression in the control group at 24 hours was not significantly higher than that of the treatment group at 24 hours ( $29.55 \pm 1.16$  vs  $29.05 \pm 1.92$ ,  $p=0.63$ ), and VEGF expression in the control group at 42 days was not significantly higher than the control group at 24 hours ( $29.58 \pm 1.21$  vs  $29.55 \pm 1.16$ ,  $p=1.00$ ). There was a difference in the expression of the VEGF expression between the control group and the treatment group (Figure 4).

After being given a secretome, it was found that VEGF expression in the treatment group at 42 days was significantly higher than the control group at 42 days ( $31.63 \pm 1.19$  vs  $29.58 \pm 1.21$ ,  $p = 0.02$ ), and VEGF expression in the treatment group at 42 days was not significantly higher than treatment group 24 hours ( $31.63 \pm 1.19$  vs  $29.05 \pm 1.92$ ,  $p=0.07$ ). There were differences in VEGF gene expression between the control and treatment groups (Figure 5).

There was an increase in VEGF gene expression where the treatment group was significantly higher than the control group with  $p < 0.05$  ( $3.33 \pm 0.59$  vs  $0.93 \pm 1.28$   $p = 0.01$ ), indicating that there was an effect of secretome administration between the control group and treatment group on increasing VEGF expression in fecal incontinence.

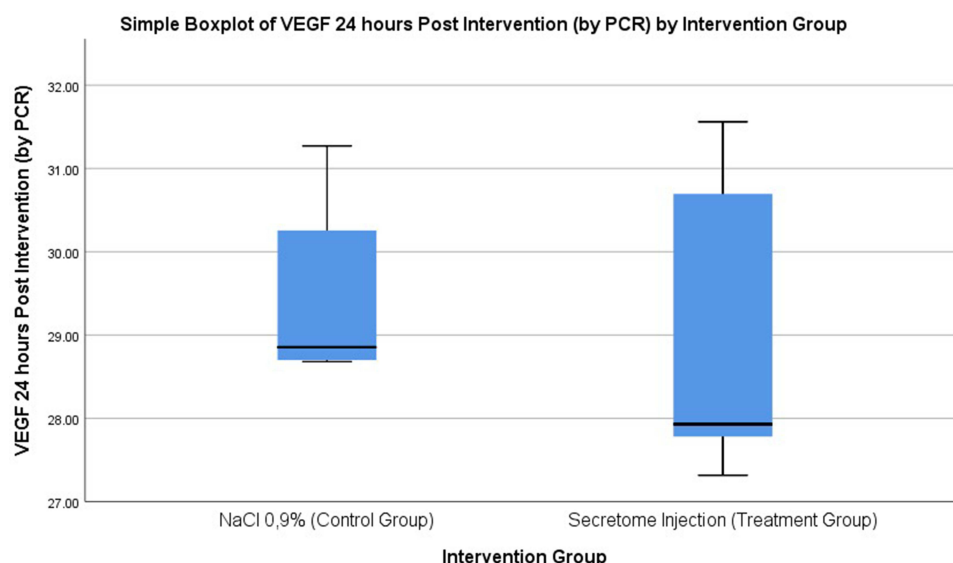


**Figure 4** VEGF expression in 24 hours Control Group (left) Treatment Group (right).

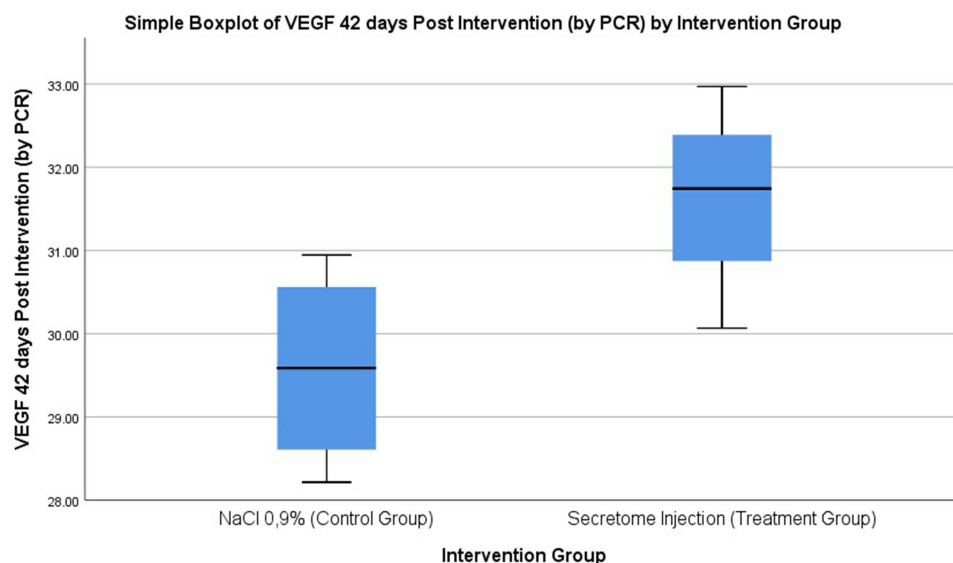


**Figure 5** VEGF expression in 42 days Control Group (left) Treatment Group (right).

After being given a secretome, it was found that neovascularization in the treatment group 24 hours later was significantly higher than in the control group ( $3.60 \pm 0.54$  vs  $2.20 \pm 0.83$ ,  $p=0.014$ ), and neovascularization in the treatment group 42 days later was considerably lower than in the control group ( $1.50 \pm 1.00$  vs  $3.00 \pm 0.00$ ,  $p: 0.024$ ). There were differences in neovascularization between the control and treatment groups (Table 1, Figures 6–9). There was an increase in neovascularization where the treatment group was significantly higher than the control group with  $p < 0.05$  ( $3.0000 \pm 1.41$  vs  $-0.5000 \pm 0.58$   $p = 0.004$ ), indicating that there was an effect of secretome administration between the control group and treatment group on increasing neovascularization in fecal incontinence rats.

The study revealed that at 24 hours, rats with fecal incontinence in the treatment group had higher fibroblast scores than those in the control group ( $1.80 \pm 0.44$  vs  $1.20 \pm 0.44$ ). By 42 days, the fibroblast score in the treatment group was also higher than in the control group ( $2.25 \pm 0.50$  vs  $1.75 \pm 0.50$ ), suggesting that secretome administration has a beneficial effect in increasing fibroblast in the fecal incontinence rats (Table 1).

**Table 1** Comparative Assessment of Neovascularization, Fibrosis and Fibroblast in 24 hours and 42 Days Post-Administration of NaCl 0.9% Vs Hypoxic Secretome Intervention

Parameter	NaCl 0.9%		Hypoxic Secretome	
	Mean (SD)	Med (Min–Max)	Mean (SD)	Med (Min–Max)
<b>24 hours</b>				
Neovascularization	2.20 (0.83)	2.00 (1.00–3.00)	3.60 (0.54)	3.00 (3.00–4.00)
Fibrosis	1.00 (0.00)	1.00 (1.00–1.00)	3.80 (0.44)	4.00 (3.00–4.00)
Fibroblast	1.20 (0.44)	1.00 (1.00–2.00)	1.80 (0.44)	2.00 (1.00–2.00)
<b>42 days</b>				
Neovascularization	3.00 (0.00)	3.00 (3.00–3.00)	1.50 (1.00)	1.50 (1.00–3.00)
Fibrosis	2.25 (0.95)	2.50 (1.00–3.00)	4.00 (0.00)	4.00 (4.00–4.00)
Fibroblast	1.75 (0.50)	2.00 (1.00–2.00)	2.25 (0.50)	2.00 (2.00–3.00)

After being given a secretome, it was found that the fibrosis score of fecal incontinence rats in the treatment group at 42 days was significantly higher than the control group at 42 days ( $4.00 \pm 0.00$  vs  $2.25 \pm 0.95$ ,  $p=0.03$ ) and fibrosis scores in treatment group 24 hours was significantly higher than control group 24 hours ( $3.80 \pm 0.44$  vs  $1.00 \pm 0.00$ ,  $p = 0.00$ ) and

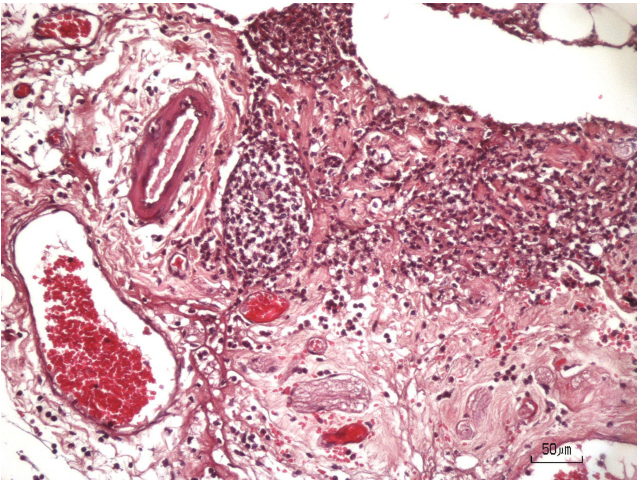


**Figure 6** Tissue Angiogenesis in the Group with Secretome Intervention – 24 hours Post Intervention (Score:  $2.20 \pm 0.83$ ).

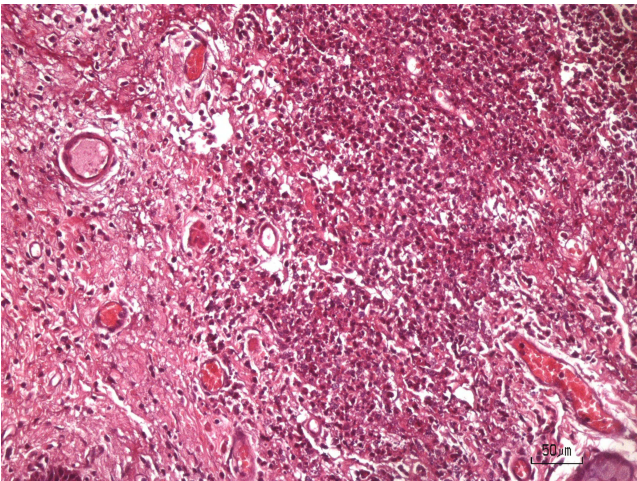


**Figure 7** Tissue Angiogenesis in the Group with NaCl 0.9% Intervention – 24 hours Post Intervention (Score:  $3.60 \pm 0.54$ ).



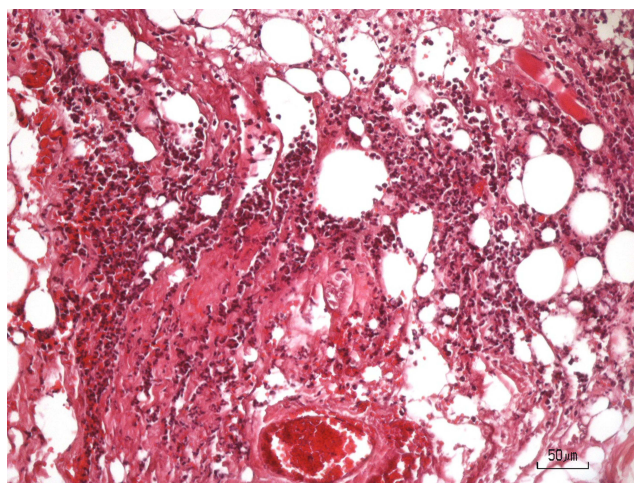


**Figure 8** Vascular Feature in the Group with Secretome Intervention – 42 days Post Intervention (Score:  $3.00 \pm 0.00$ ).

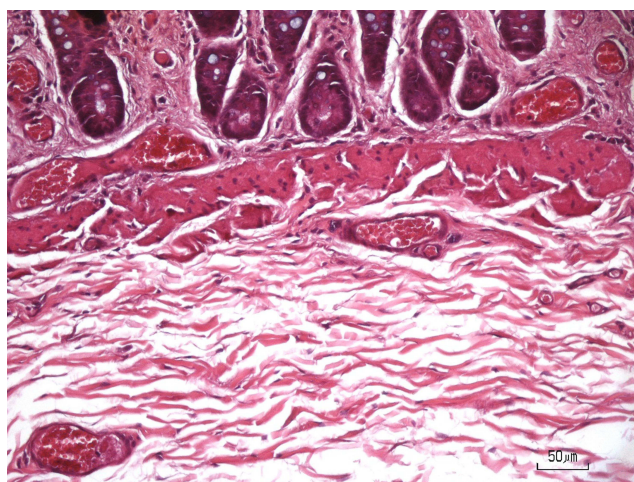


**Figure 9** Vascular Feature in the Group with NaCl 0.9% Intervention – 42 days Post Intervention (Score:  $1.50 \pm 1.00$ ).

found that the fibrosis score in treatment group 42 days was not significantly higher compared with treatment group 24 hours ( $4.00 \pm 0.00$  vs  $3.80 \pm 0.44$ ,  $p=0.31$ ). There was a difference in fibrosis scores between the control and treatment groups (Table 1, Figures 10–13). There was an increase in Fibrosis score where the treatment group was significantly higher than the control group with  $p < 0.05$  ( $3.75 \pm 0.50$  vs  $2.25 \pm 0.95$ ,  $p = 0.03$ ), indicating that there was an effect of secretome administration between the control group and treatment group on increasing fibrosis score in fecal incontinence rats.

The histological assessment of collagen deposition based on Masson Trichrome staining and, with the help of Image-J software, demonstrated a difference in % collagen area and collagen area density between the NaCl 0.9% group compared to the hypoxic secretome. It was found that the collagen area ( $\mu\text{m}^2$ ) of fecal incontinence rats in the treatment group at 24 hours was lower than in the control group at 24 hours ( $380.257,77 \pm 126.408,72$  vs  $405.794,55 \pm 147.094,15$ ). Still, the collagen area in the treatment group at 42 days was higher than in the control group at 42 days ( $799.285,43 \pm 222.363,21$  vs  $592.488,71 \pm 148.736,27$ ). After being given secretome, it was found that there was a higher increase in collagen area in the treatment group compared to the control group ( $419.027,66$  vs  $186.694,16$ ), indicating that there was an effect of secretome administration between the treatment group and control group on increasing the collagen area in fecal incontinence rats (Table 2; Figures 14–19).

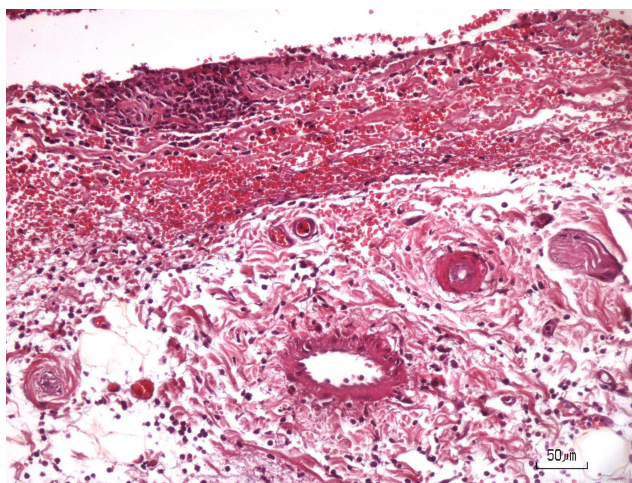


**Figure 10** Fibrosis Feature in the Group with Secretome Intervention – 24 hours Post Intervention (Score:  $3.80 \pm 0.44$ ).

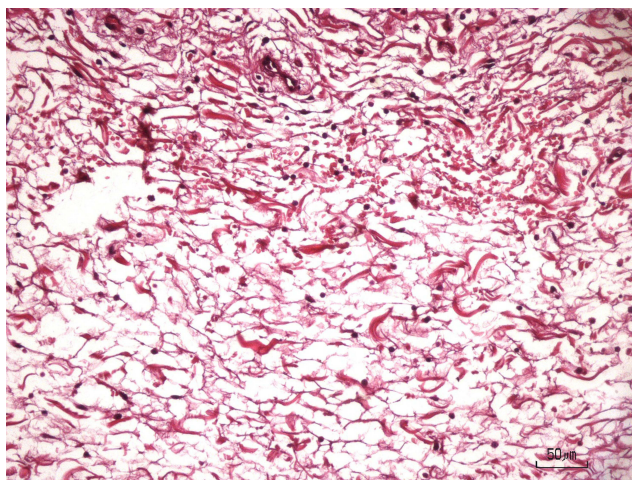


**Figure 11** Fibrosis Feature in the Group with NaCl 0.9% Intervention – 24 hours Post Intervention (Score:  $1.00 \pm 0.00$ ).

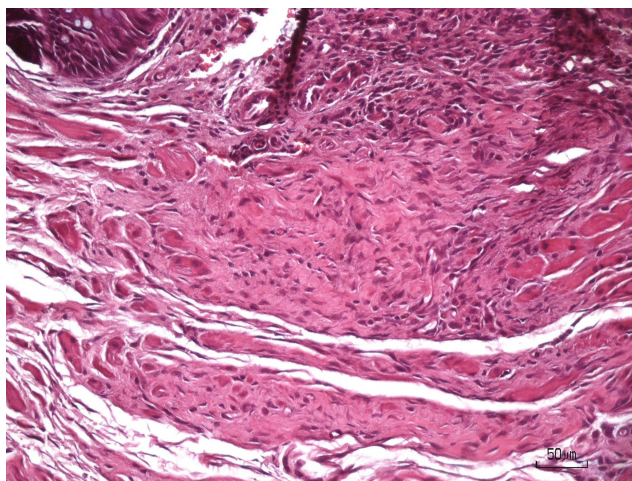


**Figure 12** Fibrosis Feature in the Group with Secretome Intervention – 42 days Post Intervention (Score:  $4.00 \pm 0.00$ ).



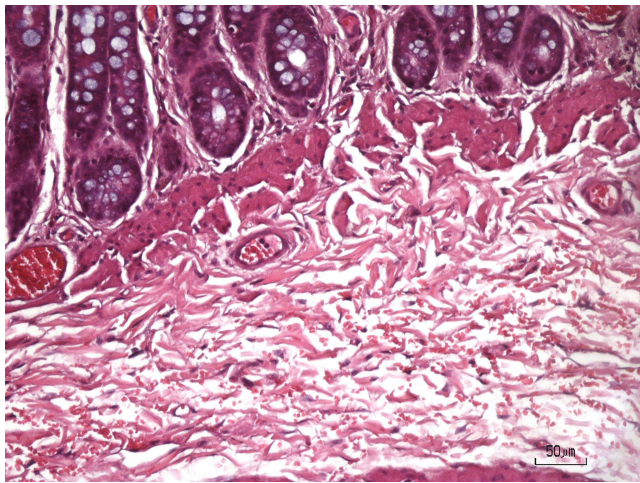


**Figure 13** Fibrosis Feature in the Group with NaCl 0.9% Intervention – 42 days Post Intervention (2.25±0.95).

The study showed that the % collagen area in the treatment group at 24 hours was lower than in the control group at 24 hours (41.03 ± 12.33 vs 45.06 ± 8.46), but the % collagen area in the treatment group at 42 days was higher than in the control group at 42 days (68.80 ± 8.96 vs 56.07±6.58). After being given secretome, it was found that there was a higher increase in % collagen area in the treatment group compared to the control group (27.77 vs 11.01), indicating that there was an effect of secretome administration between the treatment group and control group on the increase % collagen area in fecal incontinence rats. (Table 2; Figures 16–21)

Discussion

In general, the wound healing process consists of three phases: the inflammation phase, the proliferation phase, and the maturation phase. The wound-healing process involves both biomolecular and cellular responses. The expression of the HIF-1α gene is a biomolecular response that occurs due to trauma and plays a role in neovascularization.<sup>26,27</sup> HIF-1α acts as a stimulus for inducing angiogenic responses and the expression of various genes, including VEGF, one of HIF-1α’s target genes. VEGF is one of the most potent angiogenic factors and plays a role in inducing transcription in the neovascularization processes, both in physiological and pathological conditions. In the proliferation phase, fibroblasts are produced and function in cell migration and extracellular matrix formation, thereby playing a significant role in angiogenesis.<sup>26–28</sup>

Stem cell therapy is a new method to repair or replace damaged tissues and organs based on the proliferation and differentiation of transplanted stem cells. The main idea of stem cell therapy is to harness the amazing ability of stem

**Table 2** Comparative Assessment of Collagen in 24 hours and 42 Days Post-Administration of NaCl 0.9% Vs Hypoxic Secretome Intervention

Parameter	NaCl 0.9%		Hypoxic Secretome	
	Mean (SD)	Med (Min–Max)	Mean (SD)	Med (Min–Max)
<b>24 hours</b>				
% Collagen Area	45.06 (8.46)	42.05 (36.21–54.18)	41.03 (12.33)	42.53 (22.66–52.69)
Collagen Area (μm <sup>2</sup> )	405.794,55 (147.094,15)	416.430,5 (201.939,88–609.614,38)	380.257,77 (126.408,72)	405.002,75 (246.917,25–546.144,13)
<b>42 days</b>				
% Collagen Area	56.07 (6.58)	58.09 (46.82–61.28)	68.80 (8.96)	67.72 (59.93–79.86)
Collagen Area (μm <sup>2</sup> )	592.488,71 (148.736,27)	647.891,62 (377.018,63–697.153)	799.285,43 (222.363,21)	798.298,87 (530.018,63–1.070.525.37)

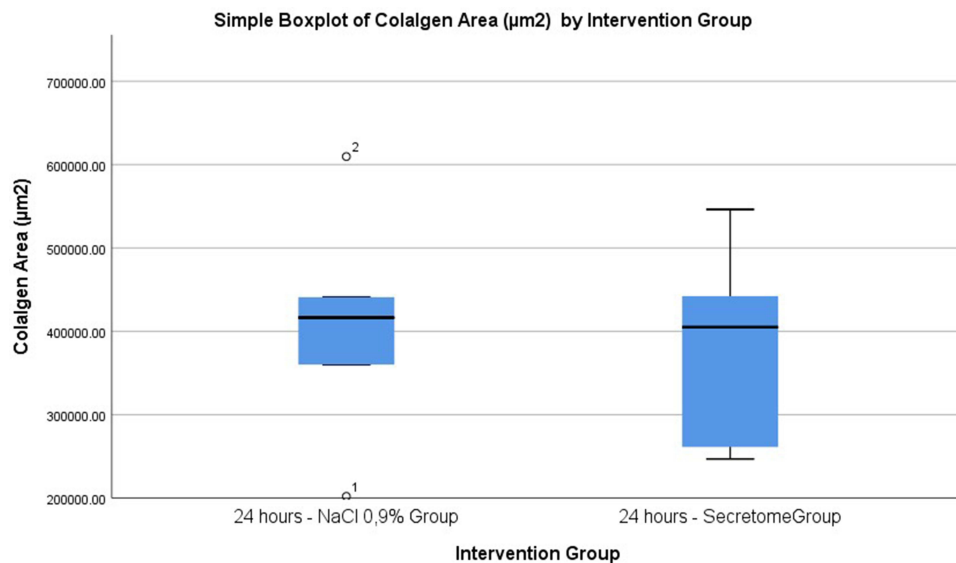


**Figure 14** Collagen Area with Masson Trichrome Staining in 24 hours Control Group (left) Treatment Group (right).

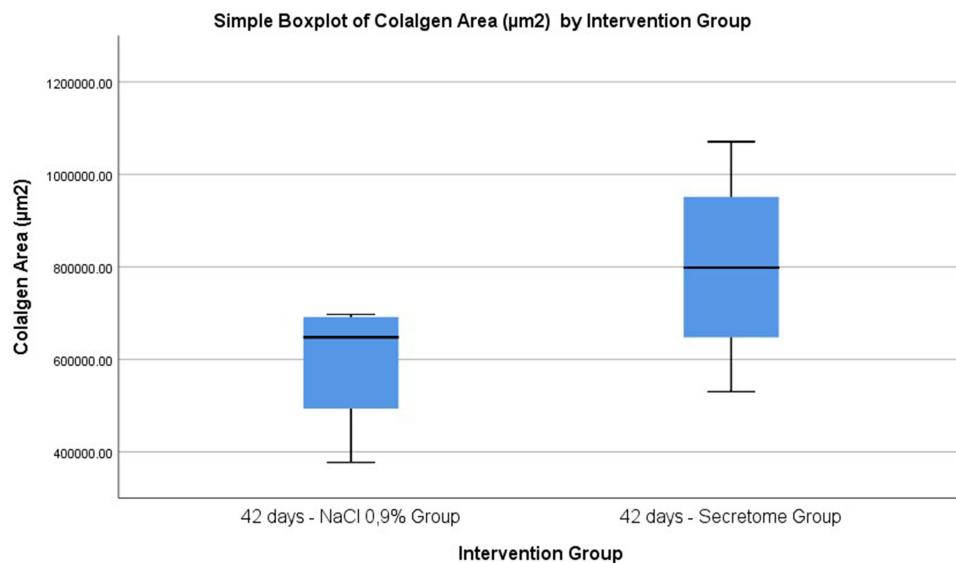


**Figure 15** Collagen Area with Masson Trichrome Staining in 42 days Control Group (left) Treatment Group (right).

cells to divide and transform into the numerous cell types required for tissue repair. When these stem cells are transplanted into the damaged area, they mature and specialize into the exact cell types required to reconstruct the damaged tissue, supporting healing and recovery. Stem cell therapy aims to restore function by repairing damaged tissues.<sup>29–31</sup>

The secretome consists of non-tumorigenic growth factors from MSCs, modulating the immune system and stimulating angiogenesis. The administration of MSC-derived secretomes plays a role in regulating both pro- and anti-inflammatory cytokines.<sup>32,33</sup> The secretome comprises several cytokines, including Tumor Growth Factor-beta (TGF- $\beta$ ), Vascular Endothelial Growth Factor (VEGF), and Insulin-Like Growth Factor-I, which can influence cell characteristics and regeneration, as well as synergistically affect migration and angiogenesis.<sup>27</sup> Additionally, the administration of secretomes can decrease the production of inflammatory cytokines such as Interleukin (IL)-6 and IL-8.<sup>27,32–34</sup> Reduced oxygen levels in various tissues activate hypoxia-inducible factor (HIF-1 $\alpha$ ), expressing angiogenic factors such as

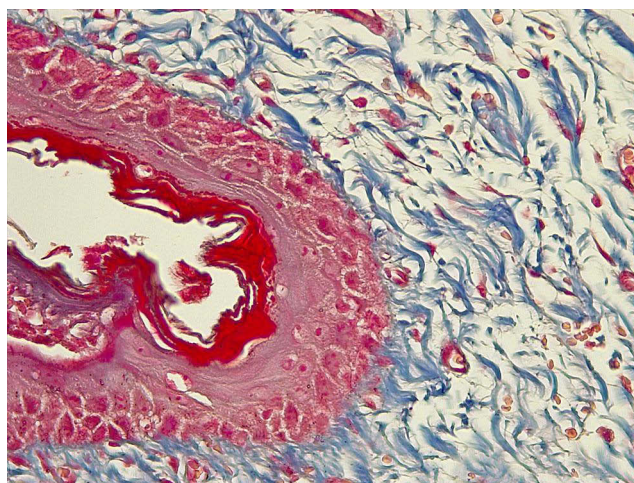


**Figure 16** Collagen Feature – 24 hours Post NaCl 0.9% Intervention.

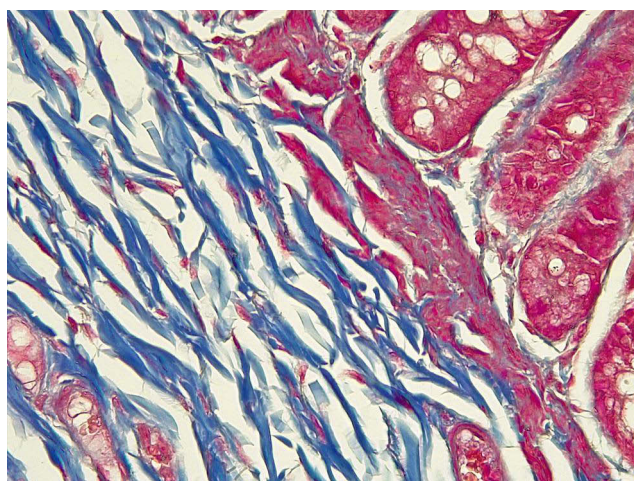


**Figure 17** Collagen Feature – 24 hours Post Hypoxic Secretome Intervention.

VEGF.<sup>35,36</sup> Cell culture under hypoxic conditions is known to have beneficial effects on MSCs, and several growth factors increase their levels in various types of stem cells under hypoxic conditions.<sup>37,38</sup>

During normal conditions, HIF-1 $\alpha$  will hydroxylate by the prolyl hydroxylase domain (PHD), leading to its degradation because of the interaction with von the Hippel–Lindau tumor suppressor protein (pVHL). But HIF-1 $\alpha$  is stable in hypoxic conditions, translocated to the nucleus, and binds with HIF-1 $\beta$  to form the active transcription factor HIF-1 that will interact with coactivator p300/CBP and binds to the hypoxia-responsive elements (HRE) to induce the transcription of target genes included VEGF (Figure 22).<sup>39</sup>

The increased expression of the HIF-1 $\alpha$  gene with the administration of hypoxic secretome in the fecal incontinence rat model can occur through the Reactive Oxygen Species (ROS) pathway, cytokines, and growth factors. In the ROS pathway, PI-3K/Akt activation leads to increased expression of the HIF-1 $\alpha$  gene. The increased expression of the HIF-1 $\alpha$  gene in the cytoplasm of the fecal incontinence rat model also results in increased expression of the VEGF protein. This



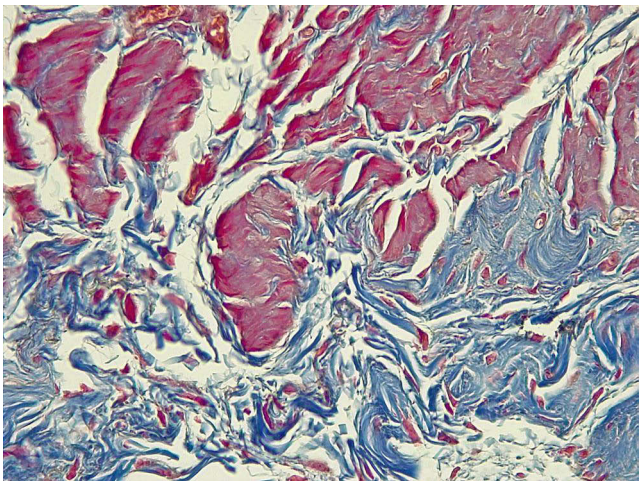


Figure 18 Collagen Feature – 42 days Post NaCl 0.9% Intervention.

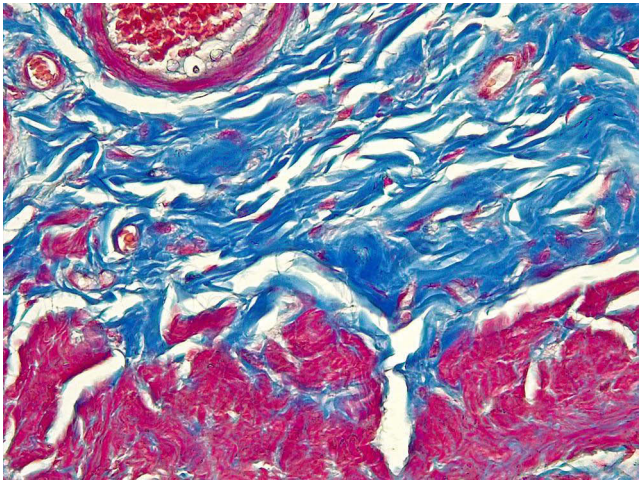


Figure 19 Collagen Feature – 42 days Post Hypoxic Secretome Intervention.

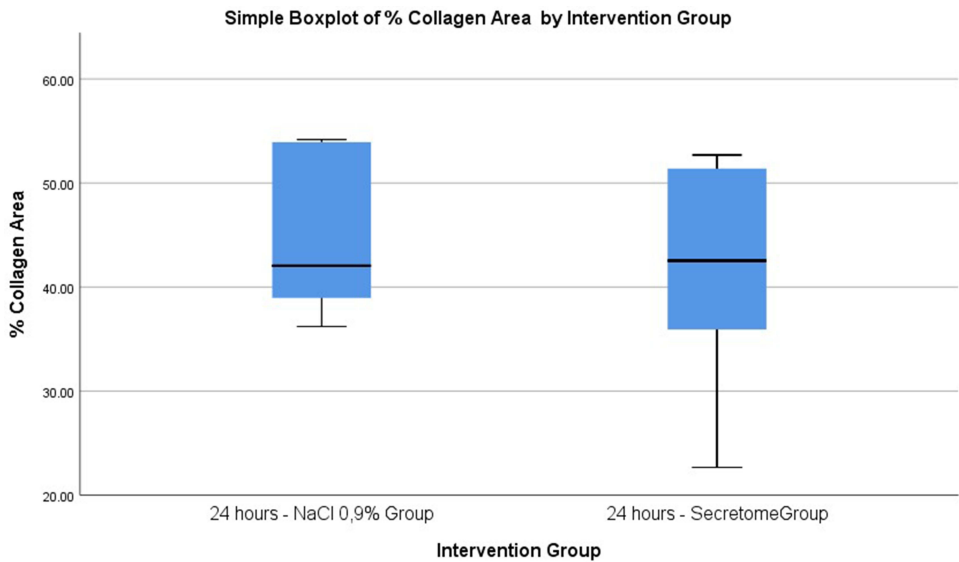
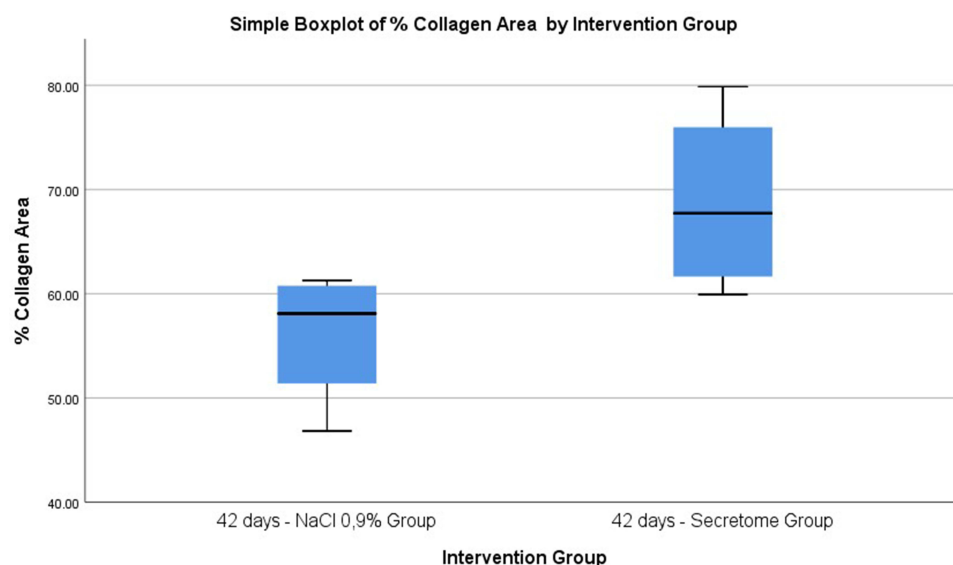
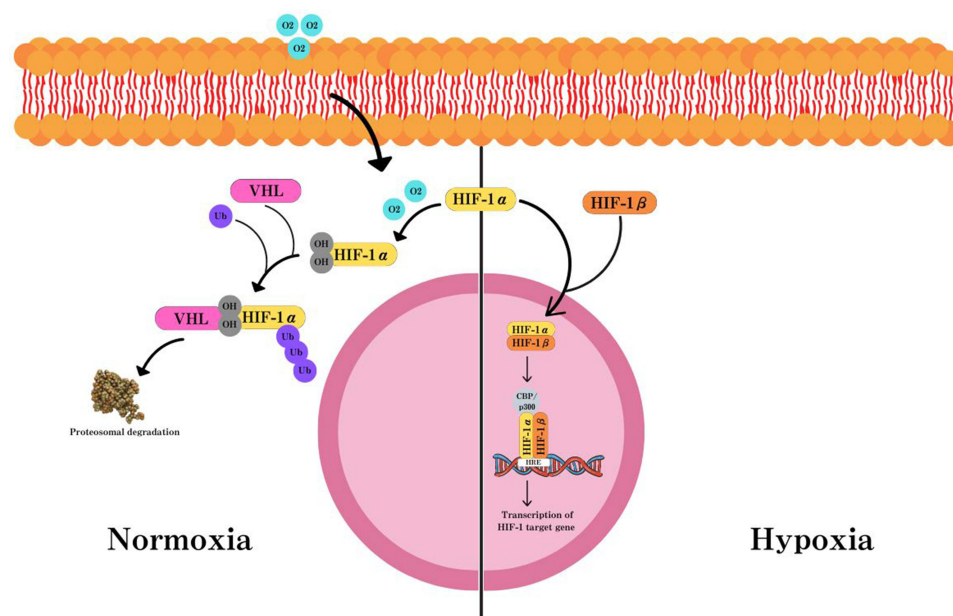


Figure 20 % Collagen Area with Masson Trichrome Staining in 24 hours Control Group (left) Treatment Group (right).



**Figure 21** % Collagen Area with Masson Trichrome Staining in 42 days Control Group (left) Treatment Group (right).



**Figure 22** Hypoxia-Inducible Factor 1 (HIF-1) Pathway.

elevated expression of VEGF protein leads to increased neovascularization and fibroblast formation in a fecal incontinence rat model.<sup>40,41</sup>

VEGF, also known as VEGF-A, is the most potent regulator of angiogenesis, specifically targeting endothelial cells.<sup>37</sup> It's part of a gene family that includes placenta growth factor (PlGF), VEGF-B, VEGF-C, and VEGF-D.<sup>42</sup> In hypoxic conditions, the VEGF gene is activated due to increased accumulation of HIF-1 $\alpha$ , an oxygen sensor, to stimulate angiogenesis and improve oxygen delivery. The HIF-1 complex binds to the VEGF gene promoter, recruiting additional transcriptional factors like P-CREB and P-STAT3 to start VEGF transcription.<sup>37,43</sup> VEGF mRNA levels significantly rise within hours of hypoxia exposure in various cell cultures, returning to normal when oxygen levels are restored.<sup>37</sup>

The high expression of the VEGF induces an angiogenic phenotype in endothelial cells in the sphincter ani of the rat fecal incontinence model. The paracrine effects and autocrine mechanisms of hypoxic secretome modulation in the microenvironment play a role in the entire process of angiogenesis within the immune modulation balance system.<sup>44</sup> The paracrine effects following hypoxic secretome administration lead to angiogenesis by mediating various growth factors, including increased expression of the VEGF protein. The role of VEGF protein expression leads to tissue regeneration and reduces cell death. Low tissue oxygen levels induce angiogenesis.<sup>26,45</sup>

VEGF increases angiogenesis and fibrosis through cooperation with TGF- $\beta$ , thereby increasing ECM production by fibroblasts, thus directly affecting ECM synthesis.<sup>46,47</sup> Fibroblasts function to help build connective tissue and the extracellular matrix. Connective tissue provides structural support and mechanical stability to the wound area, while the extracellular matrix acts as a scaffold for the growth and development of new cells. Furthermore, fibroblasts will produce collagen. The stem cell secretome promotes fibroblast activity, generating new tissue and ensuring that tissues have the strength and elasticity they need for good healing.<sup>48,49</sup> Thus, the secretome plays a key role in promoting wound healing: it promotes fibroblast proliferation and migration via growth factors such as the VEGF angiogenic pathway, contributing to the formation of connective tissue and extracellular matrix with the strength and elasticity required for complete recovery.<sup>50,51</sup>

In this study, the MSCs used were sourced from umbilical cords. The oxygen concentration in MSCs in amniotic fluid and umbilical cords ranges from 1.5 to % 8%. This physiological oxygen concentration is lower than the 21% O<sub>2</sub> found in normoxic conditions typically used in MSC culture in the laboratory. Studies involving hypoxia conditioning on MSCs have shown varied results, possibly due to differences in hypoxic conditions across studies, where oxygen concentration values range from 1% to 7%.<sup>52,53</sup> Increasing the duration of hypoxia exposure at 2–5% oxygen concentrations can enhance proliferation rates. Hypoxia can also stabilize HIF by downregulating p16, leading to the induction of various signaling pathways within cells, including increased expression of the anti-apoptotic protein survivin, thereby promoting a better proliferation process.<sup>52</sup>

Under hypoxic conditions, VEGF expression in MSCs is upregulated, along with increased half-life and secretion of VEGF mRNA.<sup>54,55</sup> VEGF expression is associated with hypoxia-inducible factor 1 (HIF1), which increases during hypoxic conditions, thus explaining the upregulation of VEGF expression under hypoxic conditions.<sup>52,56</sup>

Hypoxic conditions lead to stabilization and induction of HIF-1 within cells, influencing Notch and Wnt/ $\beta$ -catenin signaling and cell differentiation. This protein induces the metabolism, proliferation, and multipotency of MSCs. HIF-1 degrades rapidly with the loss of hypoxic conditions due to oxygen-dependent protein degradation, with a half-life of less than one minute. This short half-life can affect the stability and expression of HIF-1 in MSCs during exposure to environmental O<sub>2</sub> concentrations during medium changes.<sup>52,57</sup>

Applying sphincterotomy alongside secretome administration boosts the expression of the HIF-1 $\alpha$  gene, which is crucial for regulating VEGF and facilitating neovascularization. This neovascularization process also involves a proliferation phase, where growth factors like FGF and TGF induce fibroblast activity, promoting migration and the formation of the extracellular matrix.<sup>58</sup>

MSCs also secrete paracrine cytokines that regulate the wound microenvironment, including collagen formation. Collagen is a fundamental extracellular matrix (ECM) component and plays a key role in wound healing. The type and amount of collagen synthesized determines the quality and characteristics of scar tissue. Controlling the accumulation of types I and III collagen in wounds is important to prevent the formation of stiff, inelastic scar tissue.<sup>59,60</sup>

In granulation tissue, fibroblasts become activated, acquire expression of  $\alpha$ -SM-actin, and become myofibroblasts. These myofibroblasts synthesize and deposit ECM components. Stimulation of myofibroblasts by TGF- $\beta$ 1 itself is influenced by mechanical forces within injured or fibrotic tissue. TGF- $\beta$ 1 binds to ECM proteins and binding proteins, providing a reservoir of latent TGF- $\beta$ 1 that can be activated during the healing and scarring processes.<sup>61</sup>

TGF- $\beta$  signaling begins with the binding of TGF- $\beta$  to its receptors. Then, TGF- $\beta$  receptor II will phosphorylate TGF- $\beta$  receptor I and allow it to phosphorylate SMAD2 and SMAD 3 proteins. These proteins form a complex associated with SMAD 4 and translocate to the nucleus. The Smad complex interacts with Smad binding elements in the nucleus, causing gene expression to increase. TGF- $\beta$  signaling affects many genes, including collagen I and III,  $\alpha$ -SMA, fibronectin, TIMPs, and periostin (Figure 23).<sup>62,63</sup>

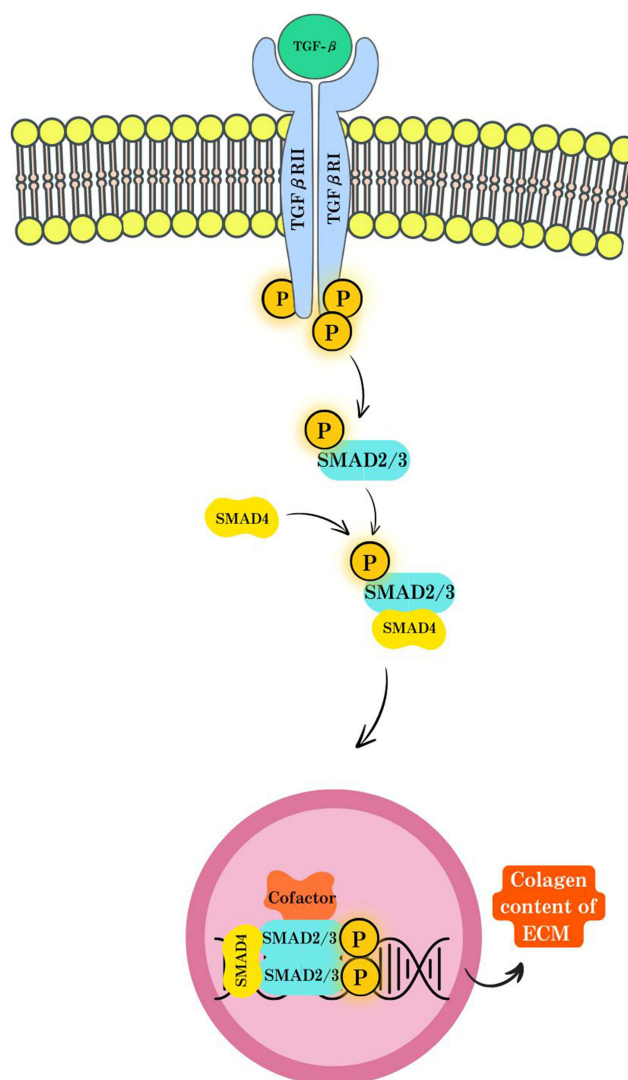


**Figure 23** Collagen Synthesis TGF- $\beta$  mediated.

This study indicates that secretome may play a role in influencing collagen accumulation by promoting the synthesis of type III collagen during the early phase of healing and the stronger type of collagen at later stages.<sup>59,60</sup> Angiogenesis is reduced, and granulation tissue is reorganized into mature scar tissue. Initially, collagen III dominates the granulation tissue but is gradually replaced by collagen I. This process involves the simultaneous formation of collagen I and degradation of collagen III, followed by remodeling of the ECM.<sup>64</sup> Even after re-epithelialization is complete, myofibroblasts in the granulation tissue continue to produce matrix metalloproteinases (MMPs) and tissue inhibitors of metalloproteinases (TIMPs). MMPs destroy certain components of the ECM, whereas TIMPs begin to inhibit MMPs when the ECM is altered, limiting further damage. Chronic wounds and abnormal changes in the ECM may result from an imbalance in the expression of TIMPs and MMPs. In contrast, fibrous scar tissue may develop if myofibroblasts do not undergo apoptosis.<sup>61,65</sup>

## Conclusions and Recommendations

The use of hypoxic secretome presents a promising therapeutic option for anal sphincter injuries post-sphincterotomy through the HIF-1 $\alpha$ -VEGF-Fibroblast signaling pathways. This approach enhances tissue repair and regeneration by modulating key factors involved in wound healing. The application of hypoxic secretome could significantly improve healing outcomes offering a novel alternative to conventional treatments in clinical practice.



## Visual Image Declaration

All images presented in this journal were entirely the original work of the author, created without plagiarism or copying from others' work. Every illustration, diagram, or visualization was independently designed by the author for this research and did not infringe upon any third-party copyright or intellectual property. We confirm that no visual material in this journal was taken from external sources without proper permission or acknowledgment.

## Abbreviation

FI, fecal incontinence; HIF-1 $\alpha$ , Hypoxia-inducible factor 1-alpha; VEGF, Vascular endothelial growth factor; PSARP, Posterosagittal Anorectoplasty; MSCs, mesenchymal stem cells; CM, conditioned medium; bFGF, basic Fibroblast Growth Factor; P-CREB, Cyclic AMP response element-binding protein; P-STAT3, Phosphorylated transducer and activator of transcription-3; mRNA, messenger RiboNucleid Acid; IACUC, Institutional Animal Care approved this experiment and Use Committees; SM-hUCMSC, secretome of human umbilical cord mesenchymal stem cells; ELISA, enzyme-linked immunosorbent assay; q-RT-PCR, Quantitative real-time reverse-transcription PCR; cDNA, complementary DNA; dT, single-stranded sequence of deoxythymine; PCR, polymerase chain reaction; RT-PCR, Reverse Transcription polymerase chain reaction; SMAD-2, Suppressor of Mothers against Decapentaplegic-2; ACTB, HUGO Gene Nomenclature Committee abbreviation; HE, hematoxylin-eosin; SPSS, Statistical Package for Social Sciences; PHD, Prolyl Hydroxylase Domain-Containing; FIH-1, Factor Inhibiting Hypoxia-1; ROS, Reactive Oxygen Species; PI-3K/Akt, phosphatidylinositol-2 Kinase; VCAM-1, Vascular cell adhesion protein 1; PDGF, Platelet-Derived Growth Factor; EGF, Epidermal Growth Factor; FGF, Fibroblasts Growth Factor; TGF- $\alpha$ , Transforming Growth Factor- $\alpha$ ; TGF- $\beta$ , Transforming Growth Factor- $\beta$ ; PGE2, prostaglandin E2; Ang-1, angiotensin-1; IL-8, Interleukin-8; TNF- $\alpha$ , Tumor Necrosis Factor- $\alpha$ ; VSMC, Vascular Smooth Muscle Cells; IL-6, Interleukin-6; PlGF, placenta growth factor.

## Data Sharing Statement

This paper has been uploaded to DataCite Commons at <https://doi.org/10.5281/zenodo.13892316>.

Data are available under the terms of the Creative Commons Attribution 4.0 International license (CC-BY 4.0).

## Ethical Declaration

This study was conducted in strict accordance with the ethical guidelines for animal research. All experimental protocols were reviewed and approved by the Institutional Animal Care and Use Committee (IACUC) of Padjadjaran University, ensuring that all procedures complied with the Animal Welfare Act and relevant ethical regulations. Every effort was made to minimize the suffering and distress of the animals, and humane endpoints were established prior to the initiation of the research. In addition to adhering to national regulations, this research complies with international standards, including the International Council for Laboratory Animal Science (ICLAS) guidelines. The care, handling, and use of the animals were in full compliance with the "3Rs" principles (Replacement, Reduction, and Refinement), ensuring the highest ethical consideration was given throughout the study.

The human umbilical cord mesenchymal stem cells used in this study were obtained with full informed consent from the donors. The donors were fully informed of the nature, purpose, and potential applications of the research, and their consent was documented in accordance with institutional guidelines. All procedures related to the collection, handling, and use of human tissue samples were conducted with the necessary permissions and in compliance with the applicable laws and ethical standards.

This study adhered to the ethical principles outlined in the Declaration of Helsinki. The research protocols were reviewed and approved by the relevant institutional ethics committee, ensuring that the rights, safety, and welfare of the donors were respected throughout the study. The confidentiality of the donors was maintained, and no identifying information was used or disclosed at any point in the research process.

## Acknowledgments

This study has been presented in the form of a self-funding presentation. The authors thank the following individuals for their generous help: Research Department, Human Research Ethics Committee Institute of Research and Community



Engagement of Padjadjaran University for ethics. The authors also acknowledge Bimana Indomedical Corporation (Bogor, Indonesia); Thank you to the Tarakan General Hospital for their permission to conduct this research. The authors thank the Tarumanagara Human Stem Cell Technology for the secretome production. Do not forget that we also thank all the nurses and doctors who have worked together to complete this research properly. We also thank Yohanes Firmansyah, Lavenia Quinta Saraswati, Indira Fadhila, Bryan Anna Wijaya, and Dewi Ismi Masitoh for kindly preparing the human umbilical cord mesenchymal stem cell secretome, statistics data, and mechanical testing.

## Funding

Self-funding.

## Disclosure

The authors declared that they have no conflicts of interest.

## References

- Dexter E, Walshaw J, Wynn H, et al. Faecal incontinence—a comprehensive review. *Front Surg*. 2024;11. doi:10.3389/fsurg.2024.1340720/full
- Rajindrajith S, Devanarayana NM, Thapar N, Benninga MA. Functional fecal incontinence in children. *J Pediatr Gastroenterol Nutr*. 2021;72(6):794–801. doi:10.1097/MPG.0000000000003056
- Bharucha AE, Rao SSC, Shin AS. Surgical interventions and the use of device-aided therapy for the treatment of fecal incontinence and defecatory disorders. *Clin Gastroenterol Hepatol*. 2017;15(12):1844–1854. doi:10.1016/j.cgh.2017.08.023
- Loganathan AK, Mathew AS, Kurian JJ. Assessment of quality of life and functional outcomes of operated cases of Hirschsprung disease in a developing country. *Pediatr Gastroenterol Hepatol Nutr*. 2021;24(2):145. doi:10.5223/pghn.2021.24.2.145
- Timmerman MEW, Trzpis M, Broens PMA. The problem of defecation disorders in children is underestimated and easily goes unrecognized: a cross-sectional study. *Eur J Pediatr*. 2019;178(1):33–39. doi:10.1007/s00431-018-3243-6
- Grano C, Aminoff D, Lucidi F, Violani C. Long-term disease-specific quality of life in adult anorectal malformation patients. *J Pediatr Surg*. 2011;46(4):691–698. doi:10.1016/j.jpedsurg.2010.10.016
- Bai Y, Yuan Z, Wang W, Zhao Y, Wang H, Wang W. Quality of life for children with fecal incontinence after surgically corrected anorectal malformation. *J Pediatr Surg*. 2000;35(3):462–464. doi:10.1016/S0022-3468(00)90215-X
- Sharma A, Rao SSC. Epidemiologic trends and diagnostic evaluation of fecal incontinence. *Gastroenterol Hepatol*. 2020;16(6):302–309.
- Van Koughnett JAM. Current management of fecal incontinence: choosing amongst treatment options to optimize outcomes. *World J Gastroenterol*. 2013;19(48):9216. doi:10.3748/wjg.v19.i48.9216
- Putri GY, Wahid TBOR, Masdar H. Angka Keberhasilan Posterosagittal Anorectoplasty (Psarp) yang Dinilai dari Skor Klotz pada Pasien Malformasi Anorektal Di Bangsal Bedah RSUD Arifin Achmad Provinsi Riau Periode Januari 2009–Desember 2014. *Jurnal Online Mahasiswa Fakultas Kedokteran Universitas Riau*. 2014;1(2):1–8. Indonesian.
- Burgers R, Reitsma JB, Bongers MEJ, de Lorijn F, Benninga MA. Functional nonretentive fecal incontinence: do enemas help? *J Pediatr*. 2013;162(5):1023–1027. doi:10.1016/j.jpeds.2012.10.037
- Haddad M, Besson R, Aubert D, et al. Sacral neuromodulation in children with urinary and fecal incontinence: a multicenter, open label, randomized, crossover study. *J Urol*. 2010;184(2):696–701. doi:10.1016/j.juro.2010.03.054
- Gangopadhyay AN, Pandey V, Gupta DK, Sharma SP, Kumar V, Verma A. Assessment and comparison of fecal continence in children following primary posterior sagittal anorectoplasty and abdominoperineal pull through for anorectal anomaly using clinical scoring and MRI. *J Pediatr Surg*. 2016;51(3):430–434.
- Eleuteri S, Fierabracci A. Insights into the secretome of mesenchymal stem cells and its potential applications. *Int J Mol Sci*. 2019;20(18):4597. doi:10.3390/ijms20184597
- Ahangar P, Mills SJ, Cowin AJ. Mesenchymal stem cell secretome as an emerging cell-free alternative for improving wound repair. *Int J Mol Sci*. 2020;21(19):7038.
- Song TJ. Molecular mechanism of HIF-1-independent VEGF expression in a hepatocellular carcinoma cell line. *Int J Mol Med*. 2011;28(3):449–454. doi:10.3892/ijmm.2011.719
- Hong WX, Hu MS, Esquivel M, et al. The role of hypoxia-inducible factor in wound healing. *Adv Wound Care*. 2014;3(5):390–399. doi:10.1089/wound.2013.0520
- Li X, Zhang D, Yu Y, Wang L, Zhao M. Umbilical cord-derived mesenchymal stem cell secretome promotes skin regeneration and rejuvenation: from mechanism to therapeutics. *Cell Prolif*. 2024;57(4). doi:10.1111/cpr.13586
- Semenza GL, Neufeldt MK, Chi SM, Antonarakis SE. Hypoxia-inducible nuclear factors bind to an enhancer element located 3' to the human erythropoietin gene. *Proc Natl Acad Sci*. 1991;88(13):5680–5684. doi:10.1073/pnas.88.13.5680
- Arsenijevic T, Grégoire F, Delforge V, Delpote C, Perret J. Murine 3T3-L1 adipocyte cell differentiation model: validated reference genes for qPCR gene expression analysis. *PLoS One*. 2012;7(5):e37517. doi:10.1371/journal.pone.0037517
- Bisson A, Fréret M, Drouot L, et al. Restoration of anal sphincter function after myoblast cell therapy in incontinent rats. *Cell Transplant*. 2015;24(2):277–286. doi:10.3727/096368913X674053
- Ueno T, Saito S, Rogers TT, Ralph MAL. Lichtheim 2: synthesizing aphasia and the neural basis of language in a neurocomputational model of the dual dorsal-ventral language pathways. *Neuron*. 2011;72(2):385–396.

23. Schlieve CR, Mojica SG, Holoyda KA, Hou X, Fowler KL, Grikscheit TC. Vascular Endothelial Growth Factor (VEGF) bioavailability regulates angiogenesis and intestinal stem and progenitor cell proliferation during postnatal small intestinal development. *PLoS One*. 2016;11(3):e0151396. doi:10.1371/journal.pone.0151396
24. Textor JA, Clark KC, Walker NJ, et al. Allogeneic stem cells alter gene expression and improve healing of distal limb wounds in horses. *Stem Cells Transl Med*. 2018;7(1):98–108. doi:10.1002/sctm.17-0071
25. Guo HF, Mohd Ali R, Abd Hamid R, Chang SK, Zainal Z, Khaza'ai H. A new histological score grade for deep partial-thickness burn wound healing process. *Int J Burns Trauma*. 2020;10(5):218–224.
26. Gutpell KM, Hoffman LM. VEGF induces stress fiber formation in fibroblasts isolated from dystrophic muscle. *J Cell Commun Signal*. 2015;9(4):353–360. doi:10.1007/s12079-015-0300-z
27. Harrell C, Fellabaum C, Jovicic N, Djonov V, Arsenijevic N, Volarevic V. Molecular mechanisms responsible for therapeutic potential of mesenchymal stem cell-derived secretome. *Cells*. 2019;8(5):467. doi:10.3390/cells8050467
28. Cimmino F, Avitabile M, Lasorsa VA, et al. HIF-1 transcription activity: HIF1A driven response in normoxia and in hypoxia. *BMC Med Genet*. 2019;20(1):37. doi:10.1186/s12881-019-0767-1
29. Kasarla RR, Pathak L. Stem cell therapy in regenerative medicine and tissue engineering. *J Stem Cell Res*. 2022;3(3):1–4. doi:10.52793/JSCR.2021.3(3)-37
30. Shingyochi Y, Orbay H, Mizuno H. Adipose-derived stem cells for wound repair and regeneration. *Expert Opin Biol Ther*. 2015;15(9):1285–1292. doi:10.1517/14712598.2015.1053867
31. Kim H, Kim Y, Park J, Hwang NS, Lee YK, Hwang Y. Recent advances in engineered stem cell-derived cell sheets for tissue regeneration. *Polymers*. 2019;11(2):209. doi:10.3390/polym11020209
32. Yu Z, Witman N, Wang W, et al. Cell-mediated delivery of VEGF modified mRNA enhances blood vessel regeneration and ameliorates murine critical limb ischemia. *J Control Release*. 2019;310:103–114. doi:10.1016/j.jconrel.2019.08.014
33. Li M, Jia Q, Chen T, Zhao Z, Chen J, Zhang J. The role of vascular endothelial growth factor and vascular endothelial growth inhibitor in clinical outcome of traumatic brain injury. *Clin Neurol Neurosurg*. 2016;144:7–13. doi:10.1016/j.clineuro.2016.02.032
34. Paruk F, Chausse JM. Monitoring the post surgery inflammatory host response. *J Emerg Crit Care Med*. 2019;3:47. doi:10.21037/jeccm.2019.08.06
35. Madrigal M, Rao KS, Riordan NH. A review of therapeutic effects of mesenchymal stem cell secretions and induction of secretory modification by different culture methods. *J Transl Med*. 2014;12(1):260. doi:10.1186/s12967-014-0260-8
36. Pawitan JA. Prospect of stem cell conditioned medium in regenerative medicine. *Biomed Res Int*. 2014;2014(1):1–14. doi:10.1155/2014/965849
37. Ahluwalia A, S Tarnawski A. Critical role of hypoxia sensor—HIF-1 $\alpha$  in VEGF gene activation. Implications for angiogenesis and tissue injury healing. *Curr Med Chem*. 2012;19(1):90–97. doi:10.2174/092986712803413944
38. Vizoso F, Eiro N, Cid S, Schneider J, Perez-Fernandez R. Mesenchymal stem cell secretome: toward cell-free therapeutic strategies in regenerative medicine. *Int J Mol Sci*. 2017;18(9):1852. doi:10.3390/ijms18091852
39. Bui BP, Nguyen PL, Lee K, Cho J. Hypoxia-inducible factor-1: a novel therapeutic target for the management of cancer, drug resistance, and cancer-related pain. *Cancers*. 2022;14(24):6054. doi:10.3390/cancers14246054
40. Fojtik P, Beckerová D, Holomková K, Šenfluk M, Rotrekl V. Both hypoxia-inducible factor 1 and MAPK signaling pathway attenuate PI3K/AKT via suppression of reactive oxygen species in human pluripotent stem cells. *Front Cell Dev Biol*. 2021;8:607444. doi:10.3389/fcell.2020.607444/full
41. Zhang Z, Yao L, Yang J, Wang Z, Du G. PI3K/Akt and HIF-1 signaling pathway in hypoxia-ischemia (Review). *Mol Med Rep*. 2018;18(4):3547–3554. doi:10.3892/mmr.2018.9375
42. Ke Q, Costa M. Hypoxia-inducible factor-1 (HIF-1). *Mol Pharmacol*. 2006;70(5):1469–1480. doi:10.1124/mol.106.027029
43. Liu YV, Semenza GL. RACK1 vs. HSP90: competition for HIF-1 $\alpha$  degradation vs. stabilization. *Cell Cycle*. 2007;6(6):656–659. doi:10.4161/cc.6.6.3981
44. Shibuya M. Vascular Endothelial Growth Factor (VEGF) and Its Receptor (VEGFR) signaling in angiogenesis: a crucial target for anti- and pro-angiogenic therapies. *Genes Cancer*. 2011;2(12):1097–1105. doi:10.1177/1947601911423031
45. Melincovici CS, Boşca AB, Şuşman S, et al. Vascular endothelial growth factor (VEGF) - key factor in normal and pathological angiogenesis. *Rom J Morphol Embryol*. 2018;59(2):455–467.
46. Kretschmer M, Rüdiger D, Zahler S. Mechanical aspects of angiogenesis. *Cancers*. 2021;13(19):4987.
47. Elbialy ZI, Assar DH, Abdelnaby A, et al. RETRACTED: healing potential of spirulina platensis for skin wounds by modulating bFGF, VEGF, TGF- $\beta$ 1 and  $\alpha$ -SMA genes expression targeting angiogenesis and scar tissue formation in the rat model. *Biomed Pharmacother*. 2021;137:111349. doi:10.1016/j.biopha.2021.111349
48. Mahmoud NN, Hamad K, Al Shibitini A, et al. Investigating inflammatory markers in wound healing: understanding implications and identifying artifacts. *ACS Pharmacol Transl Sci*. 2024;7(1):18–27. doi:10.1021/acsptsci.3c00336
49. Ridiandries A, Tan JTM, Bursill CA. The role of chemokines in wound healing. *Int J Mol Sci*. 2018;19(10):3217.
50. Kwon JW, Savitri C, An B, Yang SW, Park K. Mesenchymal stem cell-derived secretomes-enriched alginate/ extracellular matrix hydrogel patch accelerates skin wound healing. *Biomater Res*. 2023;27(1):107. doi:10.1186/s40824-023-00446-y
51. Kim JH, Green DS, Ju YM, et al. Identification and characterization of stem cell secretome-based recombinant proteins for wound healing applications. *Front Bioeng Biotechnol*. 2022;10. doi:10.3389/fbioe.2022.954682/full
52. Samal JRK, Rangasami VK, Samanta S, Varghese OP, Oommen OP. Discrepancies on the role of oxygen gradient and culture condition on mesenchymal stem cell fate. *Adv Healthc Mater*. 2021;10(6):2002058. doi:10.1002/adhm.202002058
53. Ren H, Cao Y, Zhao Q, et al. Proliferation and differentiation of bone marrow stromal cells under hypoxic conditions. *Biochem Biophys Res Commun*. 2006;347(1):12–21. doi:10.1016/j.bbrc.2006.05.169
54. Okuyama H, Krishnamachary B, Zhou YF, Nagasawa H, Bosch-Marce M, Semenza GL. Expression of vascular endothelial growth factor receptor 1 in bone marrow-derived mesenchymal cells is dependent on hypoxia-inducible factor 1. *J Biol Chem*. 2006;281(22):15554–15563. doi:10.1074/jbc.M602003200
55. Xia X, Chiu PWY, Lam PK, Chin WC, Ng EKW, Lau JYW. Secretome from hypoxia-conditioned adipose-derived mesenchymal stem cells promotes the healing of gastric mucosal injury in a rodent model. *Biochim Biophys Acta Mol Basis Dis*. 2018;1864(1):178–188. doi:10.1016/j.bbdis.2017.10.009

56. Antebi B, Rodriguez LA, Walker KP, et al. Short-term physiological hypoxia potentiates the therapeutic function of mesenchymal stem cells. *Stem Cell Res Ther.* **2018**;9(1):265. doi:10.1186/s13287-018-1007-x
57. Metsälä O, Kreutzer J, Högel H, Miikkulainen P, Kallio P, Jaakkola PM. Transportable system enabling multiple irradiation studies under simultaneous hypoxia in vitro. *Radiat Oncol.* **2018**;13(1):220. doi:10.1186/s13014-018-1169-9
58. Pittenger MF, Mackay AM, Beck SC, et al. Multilineage potential of adult human mesenchymal stem cells. *Science.* **1999**;284(5411):143–147. doi:10.1126/science.284.5411.143
59. Zhang J, Qu X, Li J, et al. Tissue sheet engineered using human umbilical cord-derived mesenchymal stem cells improves diabetic wound healing. *Int J Mol Sci.* **2022**;23(20):12697. doi:10.3390/ijms232012697
60. Hu L, Zhou J, He Z, et al. In situ-formed fibrin hydrogel scaffold loaded with human umbilical cord mesenchymal stem cells promotes skin wound healing. *Cell Transplant.* **2023**;32:09636897231156215. doi:10.1177/09636897231156215
61. Desmouliere A, Darby IA, Laverdet B, Bonté F. Fibroblasts and myofibroblasts in wound healing. *Clin Cosmet Invest Dermatol.* **2014**;7:301. doi:10.2147/CCID.S50046
62. Papageorgis P, Stylianopoulos T. Role of TGF $\beta$  in regulation of the tumor microenvironment and drug delivery (Review). *Int J Oncol.* **2015**;46(3):933–943. doi:10.3892/ijo.2015.2816
63. Xu X, Zheng L, Yuan Q, et al. Transforming growth factor- $\beta$  in stem cells and tissue homeostasis. *Bone Res.* **2018**;6(1):2.
64. Reinke JM, Sorg H. Wound repair and regeneration. *Eur Surg Res.* **2012**;49(1):35–43. doi:10.1159/000339613
65. Rodrigues M, Kosaric N, Bonham CA, Gurtner GC. Wound healing: a cellular perspective. *Physiol Rev.* **2019**;99(1):665–706. doi:10.1152/physrev.00067.2017

## Journal of Inflammation Research

Dovepress

### Publish your work in this journal

The Journal of Inflammation Research is an international, peer-reviewed open-access journal that welcomes laboratory and clinical findings on the molecular basis, cell biology and pharmacology of inflammation including original research, reviews, symposium reports, hypothesis formation and commentaries on: acute/chronic inflammation; mediators of inflammation; cellular processes; molecular mechanisms; pharmacology and novel anti-inflammatory drugs; clinical conditions involving inflammation. The manuscript management system is completely online and includes a very quick and fair peer-review system. Visit <http://www.dovepress.com/testimonials.php> to read real quotes from published authors.

Submit your manuscript here: <https://www.dovepress.com/journal-of-inflammation-research-journal>